

Simultaneous Topography and Recognition Imaging Using Force Microscopy

Cordula M. Stroh,* Andreas Ebner,* Manfred Geretschl ger,[†] G nter Freudenthaler,* Ferry Kienberger,* A. S. M. Kamruzzahan,* Sandra J. Smith-Gill,[‡] Hermann J. Gruber,* and Peter Hinterdorfer*

*Institute for Biophysics and [†]Institute of Experimental Physics, Atomic Physics and Surface Science, Johannes Kepler University of Linz, A-4040 Linz, Austria; and [‡]Basic Research Laboratory, Division of Basic Sciences, Frederick Cancer Research and Development Center, National Cancer Institute, National Institutes of Health, Frederick, Maryland 21702-1201 USA

ABSTRACT We present a method for simultaneously recording topography images and localizing specific binding sites with nm positional accuracy by combining dynamic force microscopy with single molecule recognition force spectroscopy. For this we used lysozyme adsorbed to mica, the functionality of which was characterized by enzyme immunoassays. The topography and recognition images were acquired using tips that were magnetically oscillated during scanning and contained antibodies directed against lysozyme. For cantilevers with low Q-factor (~ 1 in liquid) driven at frequencies below resonance, the surface contact only affected the downward deflections (minima) of the oscillations, whereas binding of the antibody on the tip to lysozyme on the surface only affected the upwards deflections (maxima) of the oscillations. The recognition signals were therefore well separated from the topographic signals, both in space ($\Delta z \sim 5$ nm) and time (~ 0.1 ms). Topography and recognition images were simultaneously recorded using a specially designed electronic circuit with which the maxima (U_{up}) and the minima (U_{down}) of each sinusoidal cantilever deflection period were depicted. U_{down} was used for driving the feedback loop to record the height (topography) image, and U_{up} provided the data for the recognition image.

INTRODUCTION

Fluorescence microscopy has become an important tool for localizing receptor/ligand recognition in vitro systems and in living cells (for a review, see Periasamy, 2001). However, due to its limited resolution, the recognition sites cannot be resolved on the nm scale nor can they be correlated to topography features. The atomic force microscope (AFM) (Binnig et al., 1986) can resolve nm-sized details very well and yields the greatest structural details on biological samples such as proteins, nucleotides, membranes, and cells in their native, aqueous environment (for a review, see Jena and Hoerber, 2002). In addition, due to its force detection sensitivity, it has opened the possibility of measuring inter- and intramolecular forces of biomolecules on the single molecule level (Florin et al., 1994; Lee et al., 1994; Hinterdorfer et al., 1996; Rief et al., 1997; Oberhauser et al., 1998). These capabilities lead to the development of the method described in this study, which enables us to investigate the interaction of a single ligand molecule with its cognate receptor while simultaneously recording a high resolution topography image.

Single molecular interaction forces are typically studied in force spectroscopy experiments (Evans and Ritchie, 1997; Fritz et al., 1998; Ros et al., 1998; Strunz et al., 1999; Schwesinger et al., 2000; Baumgartner et al., 2000a; Kienberger et al., 2000a; Yuan et al., 2000). An AFM tip

carrying ligands is brought in contact with a surface that contains the respective cognate receptors, so that a receptor/ligand bond is formed. This bond is subsequently broken at a characteristic measurable unbinding force by retracting the tip from the surface. In a first attempt of localizing antigenic sites via force spectroscopy, force-distance cycles using tips that were functionalized with antibodies were performed during linear lateral scans on a surface to which the cognate receptor, human serum albumin (HSA), was covalently attached (Hinterdorfer et al., 1996, 1998). Binding probabilities were determined in dependence on the lateral position, resulting in binding profiles for single HSA molecules that showed a maximum, which allowed to determine lateral positions of antigenic sites with 1.5-nm accuracy.

A complete 2-D map of forces had previously been generated to study adhesion forces of polymer surfaces and cells (Mizes et al., 1991; Radmacher et al., 1994; van der Werf et al., 1994). This measuring principle, called force volume mode, was first applied to specific ligand/receptor interactions (Ludwig et al., 1997) by performing force-distance cycles with a biotinylated tip in defined areas of a μm -sized photo-patterned streptavidin surface. Topography images were simultaneously acquired from the contact region of the force distance cycles. A higher correlation between specific molecular recognition and topography approaching the single molecule level was revealed using intercellular adhesion molecules-1 (ICAM-1) on the surface (Willemsen et al., 1998) and the cognitive antibodies on the tip. More recently, force volume was also applied to cells (Grandbois et al., 2000; Lehenkari et al., 2000; Almquist et al., 2004). Albeit exciting biological questions were

Submitted March 22, 2004, and accepted for publication May 21, 2004.

Address reprint requests to Peter Hinterdorfer, Institute for Biophysics, University of Linz, Altenbergerstr. 69, A-4040 Linz, Austria. Tel.: 43-732-2468-9265; Fax: 43-732-2468-9280; E-mail: peter.hinterdorfer@jku.at.

  2004 by the Biophysical Society

0006-3495/04/09/1981/10 \$2.00

doi: 10.1529/biophysj.104.043331

addressed in all these studies, lateral resolutions and/or data acquisition times attainable by AFM imaging modes were not achieved.

The velocity of recognition force mapping is mainly restricted by the hydrodynamic forces acting on the cantilever during force-distance cycles. The experimental time for recording a high resolution force map (512×512 pixels) is ~ 7.3 h (20 Hz sampling frequency of force-distance cycles, forth and back line scan) for commercially available cantilevers (length ~ 100 μm). Ultra-short cantilevers (length ~ 5 μm) enable $\sim 25 \times$ faster z -scans in aqueous environment (Viani et al., 1999; Schäffer et al., 2001). An even enhanced speed of recording recognition maps with 3 nm lateral resolution was recently introduced (Raab et al., 1999; Schindler et al., 2000). Raab et al. used the magnetic AC mode (MACmode) (Han et al., 1996), which is also known as gentle imaging tool for obtaining high resolution images of DNA (Han et al., 1997a,b) and soft biological membranes (Kienberger et al., 2003) in aqueous environments. A magnetically oscillated atomic force microscopy tip that carried a tethered antibody was scanned along a surface to which the antigen was bound (Raab et al., 1999) and the recognition sites were detected from the amplitude reduction arising from the antibody/antigen interactions. Since the oscillation frequency used with these cantilevers is ~ 5 kHz (slightly below the resonance frequency of the cantilever in buffer), data acquisition can be $250 \times$ faster than in conventional force mapping, and $10 \times$ faster than in force mapping using ultra-short cantilevers.

In this study, the above described method is extended to yield simultaneous acquisition of two independent maps, i.e., a topography image and a lateral map of recognition sites. The two images are recorded with nm resolution at experimental times comparable to normal AFM imaging. As receptor/ligand interaction system we used lysozyme and HyHEL5 antibody (provided by S.J.S.-G.).

MATERIALS AND METHODS

Enzyme immuno assay

The functionality of mica-bound lysozyme was tested with using an enzyme immunoassay (EIA) as described before (Hinterdorfer et al., 1998). For this, lysozyme (Sigma, Vienna, Austria) was adsorbed for 15 min at 0.3 $\mu\text{g}/\text{ml}$ in 1 mM NaCl to the mica sheets (5×5 mm²) and subsequently washed with 1 mM NaCl. Unspecific binding was blocked for 10 min with PBA (6 mg/ml BSA in PBS (150 mM NaCl, 5 mM NaH₂PO₄, pH 7.5)). Then, 200 μl of 20 $\mu\text{g}/\text{ml}$ HyHEL5 antibody (provided by S.J.S.-G.) in PBA were added to the mica sheets for 30 min and subsequently washed with PBA before 200 μl of 20 $\mu\text{g}/\text{ml}$ in PBA peroxidase conjugated anti-mouse IgG (Sigma, Vienna, Austria) was added for 30 min and subsequently washed with PBA and PBS. For control samples addition of HyHEL5 was omitted. Cuvettes containing a magnetic stirrer were filled with 3 ml 50 mM citric acid (pH = 5.5), 0.8 mg/ml phenylendiamine, and 30 μl of H₂O₂ (3%, v/v). Absorption was detected every minute at 490 nm with a Shimadzu (Shimadzu GmbH, Duisburg, Germany) spectrometer. Calibration was done with 2 μl of 20 $\mu\text{g}/\text{ml}$ peroxidase conjugated in the solution described above.

Conjugation of HyHEL5 antibody to AFM tips

Conjugation of an antibody (HyHEL5, directed against lysozyme) to AFM tips was performed using a flexible poly(ethylene glycol) (PEG) cross-linker (Haselgruebler et al., 1995; Hinterdorfer et al., 1996,1998). After drying the cross-linker-modified tips with nitrogen, they were immediately incubated in 200 μl SATP-conjugated antibody (0.13 mg/ml in buffer A) in a plastic petri dish and 40 μl (one-fifth of the total volume) of hydroxylamine reagent (see Haselgruebler et al., 1995) was added to de-protect the thiol-group of the antibody. After 1 h incubation time, the tips were extensively washed with buffer and stored at 4°C.

Sample preparation

For topography and recognition imaging, lysozyme was adsorbed to freshly cleaved mica sheets at 0.3 $\mu\text{g}/\text{ml}$ in 1 mM NaCl and washed after 15 min in 1 mM NaCl and PBS. Force spectroscopy and force mapping were carried out on a dense lysozyme layer, which was deposited by incubation with 10 to 20 $\mu\text{g}/\text{ml}$ lysozyme in 1 mM NaCl for 15 min. Subsequently, the sample was washed in 1 mM NaCl and PBS.

AFM measurements

For the detection of single antibody-antigen recognition events, force distance cycles were performed using antibody-coated cantilevers (Microlevers, Veeco, Santa Barbara, CA) with 0.01–0.03 N/m nominal spring constant in the conventional force spectroscopy mode. The vertical piezo movement was 50–150 nm at sweep rates from 1–10 Hz. For force quantification, spring constants of cantilevers were determined using the thermal noise method (Hutter and Bechhoefer, 1993; Butt and Jaschke, 1995). The analysis of the force distance cycles was performed using MATLAB (MathWorks, Natick, MA) as described (Baumgartner et al., 2000b). Blocking was done with 100 $\mu\text{g}/\text{ml}$ HyHEL5 antibody for 20–30 min.

Force volume mode images were acquired with a DI Multimode AFM connected to a Nanoscope IIIa controller (Digital Instruments, Santa Barbara, CA) using a lateral resolution of 64×64 pixels in a scan area of 250 nm. Lysozyme was adsorbed to a mica surface and the tips were modified with HyHEL5 antibody. The according force-distance cycles were obtained at 50 nm scan amplitude and 10 Hz sweep rate and saved with 64 points per curve. Lysozyme molecules on mica were blocked by addition of 53 μl 5.7 mg/ml HyHEL5 antibody into the fluid cell of the AFM and subsequent incubation for 40 min.

Topography and recognition images were recorded in the magnetic AC (MAC) mode using a PicoSPM (Molecular Imaging Corporation, Tempe, AZ) with MAC levers (Molecular Imaging Corporation, Tempe, AZ) of 0.1 N/m nominal spring constant. A lateral scan frequency of 1 line/s was employed for all topographical and simultaneously acquired topography/recognition images. Using 512 lines per image, the total recording time was 8 min. Integral and proportional gains were adjusted to optimize the sensitivity of the feedback loop; typical values were 0.3 and 0.5, respectively. Measurements were performed with 5–10 nm free tip oscillation amplitude at 7–10 kHz driving frequency and $\sim 40\%$ amplitude reduction in PBS. Sometimes, the slow scan axis was disabled and the feedback shut off, and the deflection signal was recorded on a sound card using GoldWave software (GoldWave, St. John's, NF, Canada). The x -scanning signal was also fed into the sound card and provided the time clock. Traces were analyzed using MATLAB. Blocking was done by addition of 500 μl of 1 $\mu\text{g}/\text{ml}$ HyHEL5 antibody and subsequent incubation for 30 min. For the simultaneous acquisition of separate topography and recognition images the photodetector signal was fed into a home-built electronics box and accordingly processed.

RESULTS AND DISCUSSION

Enzyme immuno assay

Fig. 1 shows the results of the enzyme immuno assay (EIA) performed to measure the antibody/lysozyme binding capability and to quantify the surface density of functional lysozymes. Samples 1 and 2 were coated with lysozyme, followed by specific binding of HyHEL5 antibody and of peroxidase-conjugated anti-mouse IgG, whereas for samples 3 and 4 binding of HyHEL5 was omitted (control). Absorbance at 490 nm was monitored to quantify the amount of bound marker enzyme (Fig. 1, cf. methods section). Absorbance values for samples incubated with HyHEL5 (samples 1, 2) were $8\text{--}10 \times$ larger than for samples lacking the primary antibody (samples 3, 4; Fig. 1 A). This clearly indicates that HyHEL5 antibodies were specifically ligated to lysozyme, which means that the mica-adsorbed lysozyme molecules were still functional. By comparison

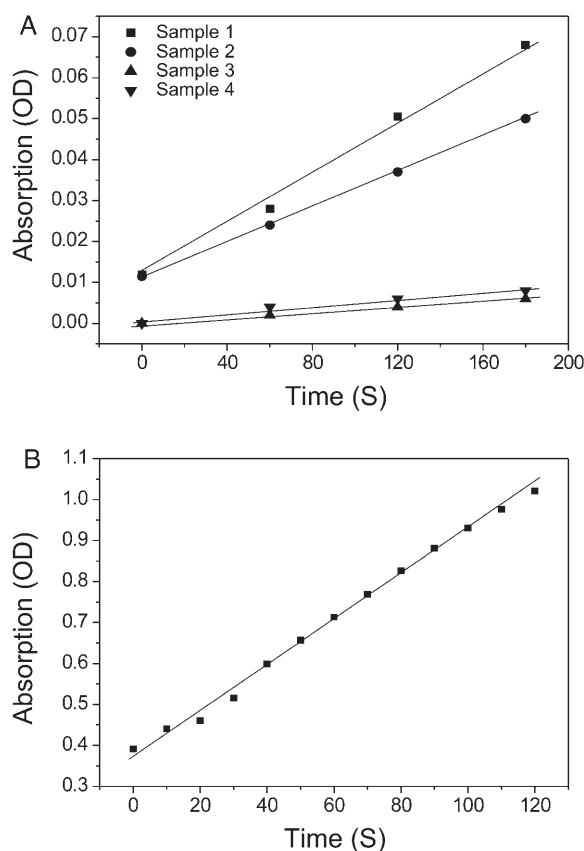


FIGURE 1 Enzyme immuno assay of HyHEL5-lysozyme binding. (A) Mica sheet 1 and 2 were successively coated with lysozyme, anti-lysozyme (HyHEL5), and peroxidase conjugated anti-mouse IgG. Sheets 3 and 4 were only coated with lysozyme and peroxidase conjugated anti-mouse IgG. The higher absorption values of samples 1 and 2 compared to samples 3 and 4 reveals the specific binding of HyHEL5 to its antigen. (B) Absorption time-scan of peroxidase conjugated anti-mouse IgG in solution used as calibration for the determination of the number density of active surface-bound lysozyme.

with the enzymatic activity of a known concentration of peroxidase conjugated anti-mouse IgG in free solution ($0.315/\text{min}$, Fig. 1 B) a number density of 215 ± 32 active (average and SD of samples 1 and 2) lysozyme molecules per μm^2 was calculated.

AFM topography imaging of lysozyme

Lysozyme was imaged with the AFM using the magnetic AC-mode (Han et al., 1996, 1997a, 1997b; Raab et al., 1999). The oscillating cantilever touches the surface intermittently, resulting in a reduction of the free oscillation amplitude due to the repulsive tip-sample interaction during contact. The amplitude reduction is held at a constant value by employing a feedback loop, which adjusts the vertical position of the cantilever-holder via piezo movements. The small oscillation amplitudes used ($5\text{--}10$ nm) guarantee for gentle tip-surface contact and minimize the destruction of the soft molecules that were adsorbed to the surface. While scanning over the surface, the cantilever follows the topography, resulting in the height image shown in Fig. 2. Singly distributed lysozyme molecules are clearly visible in Fig. 2 A, appearing with 1.5 nm in height (see cross section of Fig. 2 A). Apparently, the applied concentration of $0.3 \mu\text{g}/\text{ml}$ lysozyme (cf. Methods) resulted in a single molecule preparation. Counted were ~ 230 proteins in the presented image frame of $1 \mu\text{m}^2$ (Fig. 2 A). This value is in excellent agreement to the number of lysozymes counted in the enzyme immuno assay (215 ± 32), indicating almost every lysozyme of this single molecule preparation is active for binding to the HyHEL5 antibody.

Fig. 2 B shows an almost complete coverage of the mica surface with lysozyme molecules, resulting from incubation at a $30 \times$ higher concentration of lysozyme. The black holes visible in the image are ~ 2 nm deep and represent small areas of uncoated mica.

Single molecule lysozyme/HyHEL5-antibody interaction forces

The small spring constants of soft cantilevers and the high sensitivity of the AFM allow for measuring unbinding forces in the $10\text{--}100$ pN range, as they are typical for single molecular interactions of receptor/ligand pairs. These forces are known to depend on the loading rate (Grubmüller et al., 1996; Evans and Ritchie, 1997; Fritz et al., 1998; Merkel et al., 1999; Baumgartner et al., 2000a; Kienberger et al., 2000a; Schwesinger et al., 2000) and the energy landscape of the receptor/ligand interaction can be depicted from the spectrum (loading rate dependence) of the forces.

In Fig. 3, a typical force-distance cycle is shown, in which the cantilever deflection angle is measured as a function of the vertical position of the cantilever. HyHEL5 antibodies were coupled to the AFM tip and a dense lysozyme

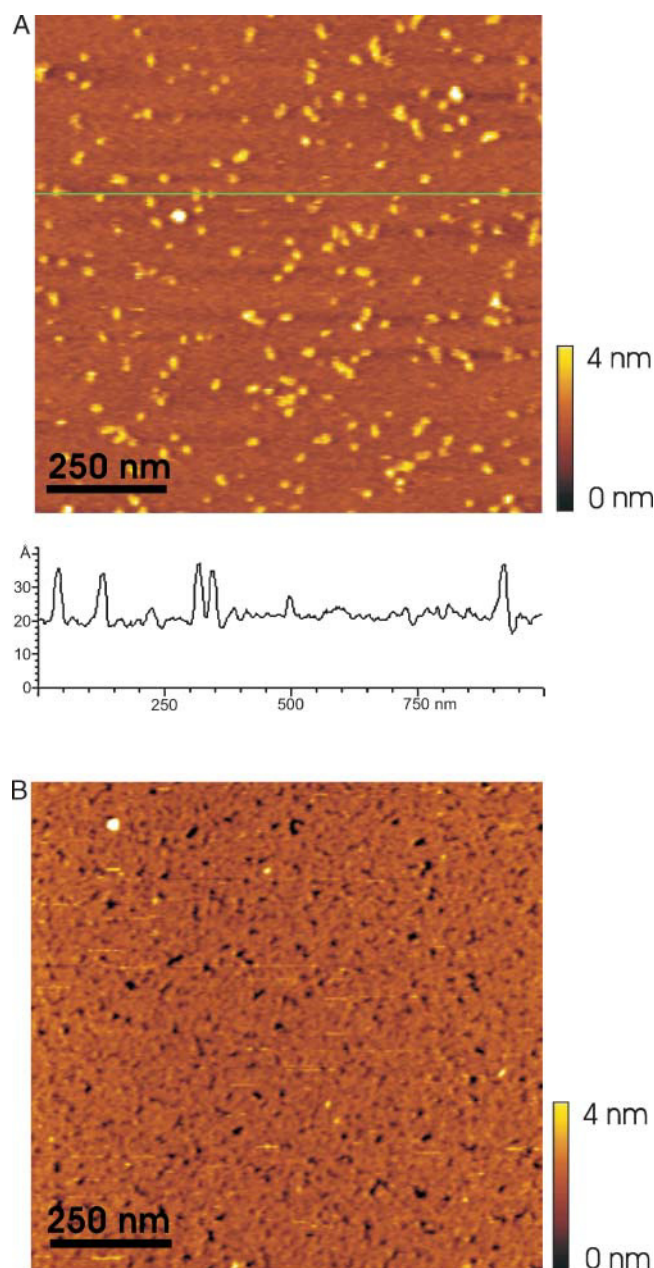


FIGURE 2 Topography images of lysozyme molecules imaged using the MAC mode. (A) Single molecule preparation. The cross section shows single lysozyme molecules with 1–2 nm in height and 15–20 nm in width. (B) A dense monolayer of lysozyme molecules adsorbed onto a mica surface as it was used for force spectroscopy experiments.

monolayer was adsorbed to the surface. First, the tip approaches the surface (trace, solid line). Far away from the surface (here: 60 to 0 nm) the cantilever deflection angle is almost zero. In the contact region (0 to –20 nm) the cantilever is bent upwards due to the repulsive tip-sample interaction developing upon contact. The measured deflection is directly proportional to the interaction force (as predicted by Hooke's law). If the antibody on the tip binds to the lysozyme adsorbed on mica, subsequent retraction

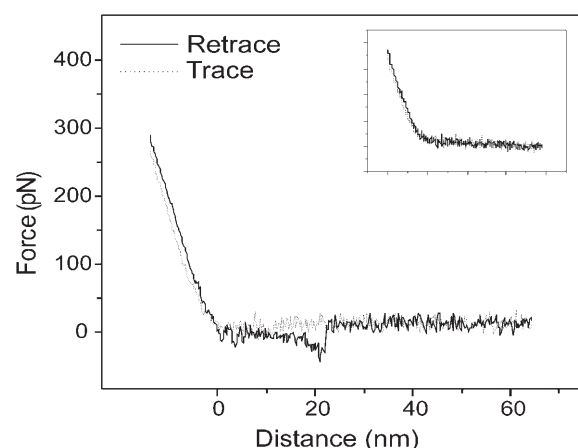


FIGURE 3 Force-distance cycle of a single molecular lysozyme-HyHEL5 unbinding event at 50 pN unbinding force and 20 nm unbinding length. Lysozyme is adsorbed onto a mica surface and the antibody HyHEL5 is attached to an AFM tip via a cross-linker molecule (PEG derivative). The inset shows a force-distance cycle measured when the binding is blocked by adding free antibody in solution.

(retrace, dotted line) of the cantilever will first result in the relaxation of the repulsive forces in the contact region (–20 to 0 nm), followed by the development of a pulling force during nonlinear stretching of the PEG tether (Kienberger et al., 2000b) (0–20 nm). Finally the antibody on the tip will unbind its antigen on the surface at a critical force, termed unbinding force. The corresponding unbinding length of 20 nm (Kienberger et al., 2000a) fits the cross-linker length (~8 nm, Riener et al., 2003) plus the size of an antibody (~12 nm, Silverton et al., 1977). The cantilever jumps back to zero deflection, and further retraction (20–60 nm) shows no more bending of the cantilever. The specificity of the binding was proven by adding free HyHEL5 antibody in solution, resulting in an effective block of the antibody/antigen interaction (inset of Fig. 3), as deduced from the absence of any unbinding event. In the majority of cases, single unbinding events as shown in Fig. 3 were observed. Multiple antibody-antigen interactions resulting in several distinguishable stretching peaks in the force-distance cycles were rarely seen, and fairly independent on the contact force. However, for simultaneous topography/recognition imaging only tips showing single unbinding events were selected.

Since a distensible cross-linker was used to couple the antibody to the AFM tip, the force-extension profile in the retrace is dominated by the force-extension characteristics of the polymer linker. As long as the polymer is relaxed, it is coiled due to maximization of entropy. Extension of the molecule then generates an opposing force. For small extensions only little force is required but the resistance to extension rises rapidly as the polymer approaches its full length (Fisher et al., 1999; Kienberger et al., 2000b). Therefore, the force exerted to the antibody/lysozyme complex increases nonlinearly and the extension curve before unbinding is of a nonlinear parabolic shape,

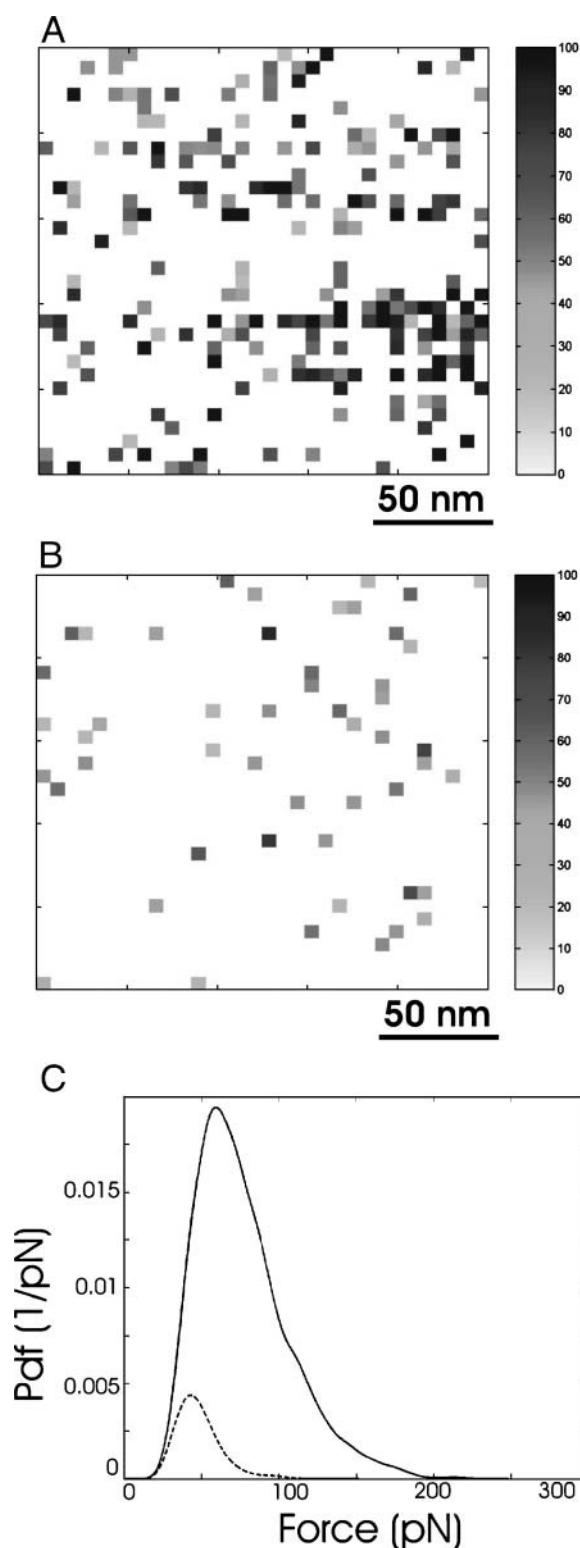


FIGURE 4 Force volume mode data using lysozyme adsorbed onto a mica surface and HyHEL5 antibody attached to the tip. Binding sites on the lysozyme layer were detected in A and significantly blocked with free HyHEL5 in solution. (B) The unbinding forces in the pixels are scaled in gray scale values (0–100 pN). (C) Pdf of the unbinding forces observed in absence (*solid line*) and in the presence of free HyHEL5 antibody (*dotted line*). Areas are scaled to binding probabilities. The most probable unbinding

approximately consistent with the behavior of a worm-like-chain model (Kienberger et al., 2000b). Due to the stretching of the cross-linker, unbinding of the complex occurs distant from the surface and is not interfered by signals arising from tip-surface interactions.

Recognition map of lysozyme recorded with force volume

Using the force volume mode, force-distance cycles were recorded in every pixel of a defined scan area of $(250 \text{ nm})^2$. Fig. 4 A shows recognition force maps derived from force distance cycles using an antibody-conjugated tip on a lysozyme layer. The unbinding forces of the individual pixels are presented in gray scale values (see *gray scale bar*, 0–100 pN). Many binding sites on the lysozyme layer were detected, yielding an overall binding probability of 20% (i.e., 20 out of 100 force distance cycles showed an unbinding event). After blocking (Fig. 4 B), the binding probability dropped dramatically. Therefore the observed interactions between HyHEL5 antibody on the tip and lysozyme molecules on the surface are based on specific molecular recognition. The force map (Fig. 4 A) indicates the lateral positions of active lysozyme molecules on the surface. However, lateral resolution of single molecules was not achieved with this mode.

Measured unbinding forces were analyzed and empirical probability density functions (pdf's) were constructed from the unbinding force values (Fig. 4 C, *solid line*). The maximum of the distribution ($\sim 60 \text{ pN}$) reflects the most probable unbinding force at the loading rate used. Upon blocking, binding probabilities were dramatically reduced, as evident by the comparison of the pdf's before (Fig. 4 C, *solid line*) and after blocking (Fig. 4 C, *dotted line*); the area of the pdf before blocking is normalized to 1 and the ratio of the areas of the two pdf's equals the ratio of binding probabilities.

Dynamic force microscopy traces

The nature of the topography and of the recognition signals appearing in dynamic force microscopy was first investigated by one-dimensional linear scans. For this, lysozyme molecules were adsorbed onto mica at surface concentrations where they were singly distributed. The sample was scanned with an oscillating cantilever carrying an antibody directed against lysozyme using the constant height mode (amplitude feedback switched off). The cantilever response was recorded during the lateral scans, from which a cutout of 4 ms is shown in Fig. 5 A. As expected, the cantilever oscillated in a sinusoidal fashion in z -direction according to

force for the specific HyHEL5-lysozyme interaction was $\sim 60 \text{ pN}$ (*solid curve*), whereas unspecific adhesion forces were slightly lower (*dotted curve*).

the preset frequency (7 kHz) and amplitude (5 nm, peak-to-peak). However, both the maxima and minima of the oscillation periods were not strictly constant, instead they changed due to the interaction between tip and sample (Fig. 5 A).

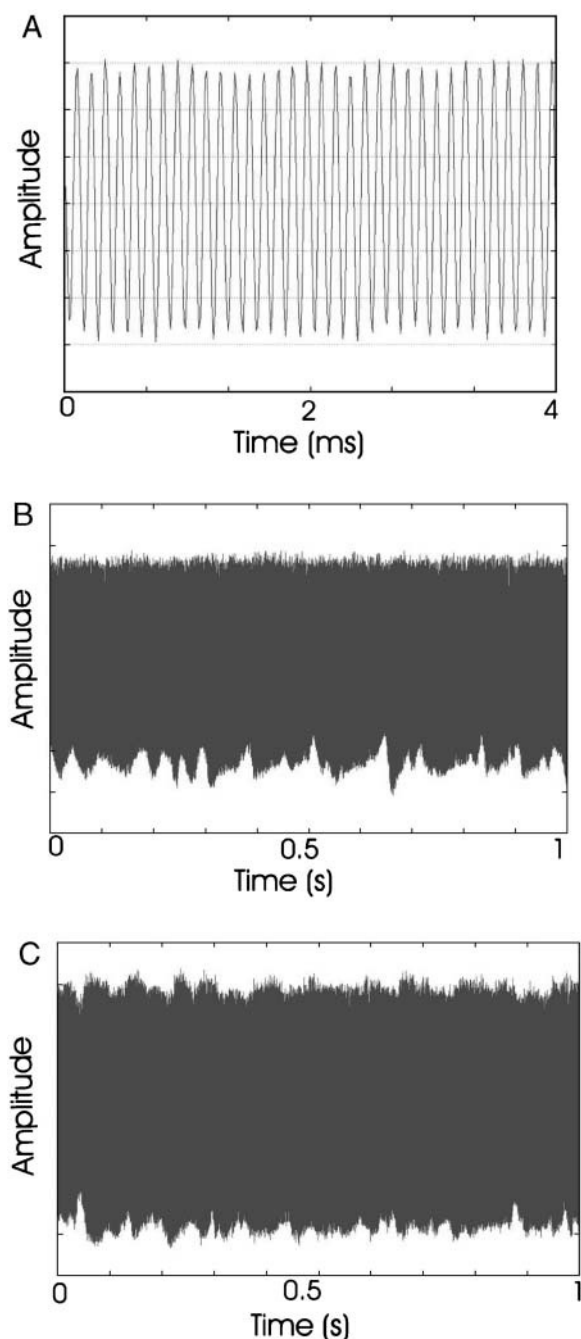


FIGURE 5 (A) Deflection signal of a magnetically oscillated cantilever during scanning along the surface when the feedback was switched off. The signal was recorded on a sound card over a time range of 4 ms. Peak to peak amplitude was 5 nm. (B) and (C) Signal as shown in A over a full scan line (500 nm scanned in 1 s). Due to the resulting compression of the time axis, only the extrema of the oscillation periods remain visible. (B) Bare tip on lysozyme molecules adsorbed onto a mica surface. (C) HyHEL5-antibody coated tip on lysozyme molecules.

In a presentation of significant larger time spans of these traces (1 s, corresponding to one full scan line of 500 nm) the oscillations appeared highly compressed and only the envelope with the characteristic maxima and minima of each oscillation period remained visible (Fig. 5, B and C). Fig. 5 B is the result of a scan with a bare tip, i.e., a tip containing no antibody. The z -positions of the minima varied significantly, and as a result singly distributed bulges with 10–15 nm width and ~ 1 nm in apparent height appeared along the scan axis. These bulges reflect single lysozyme molecules that resist the further downward movement of the tip toward the mica surface. Their widths and heights are a measure of the apparent molecule size (10–15 nm width, ~ 1 nm height), and their separation is a measure of the distance between the molecules on the surface (~ 35 nm on average). In contrast, the positions of the oscillation maxima remained constant aside from the minor randomly occurring variations caused by the thermal noise of the cantilever. Apparently, the information of the surface topography measured with a bare tip is solely contained in the minima of the cantilever oscillations and cross talk between minima and maxima does not exist at the conditions used (cantilever spring constant 0.1 N/m; Q-factor ~ 1 ; resonance frequency ~ 7 kHz) (Lantz et al., 1999). Cantilevers with higher spring constants (e.g., 0.5 N/m) have Q-factors significantly larger than one ($Q \sim 3$) and were therefore not employed for simultaneous topography/recognition imaging. In contrast, cantilevers showing higher force sensitivity (e.g., 0.03 N/m) were not used because of their low resonance frequencies (~ 3 kHz) resulting in slow imaging speeds. Additionally, low spring-constant levers show in general less stability in MACmode imaging (Kienberger et al., 2003). Thus, 0.1 N/m cantilevers with a Q-factor of ~ 1 appeared to be the best choice for sensitive and robust topography/recognition imaging.

Distinct minima were also clearly detected with an AFM tip carrying a specific antibody (Fig. 5 C), indicating that the topography information can also be obtained using these chemically modified tips. In addition, however, the maxima were significantly affected, too (Fig. 5 C). The antibody of the AFM tip binds to the specific antigenic sites on lysozyme during scanning and the physical connection thereby temporarily established between tip and substrate reduces the upstroke of the cantilever oscillation. As a further consequence, recognition of lysozyme by the tip-conjugated antibody results in reduction of the oscillation maxima, which allows for detection of the lateral position of specific binding sites.

Values of minima and maxima during repetitive linear scans are shown (Fig. 6). In Fig. 6 A the principle of recording is depicted. The tip was approached to the surface (Fig. 6 A, upper left corner of the image) using the MAC mode and scanned from the left to the right (fast scan axis). The scan was continued by a line-by-line down-movement (slow scan axis). Single lysozyme molecules appearing

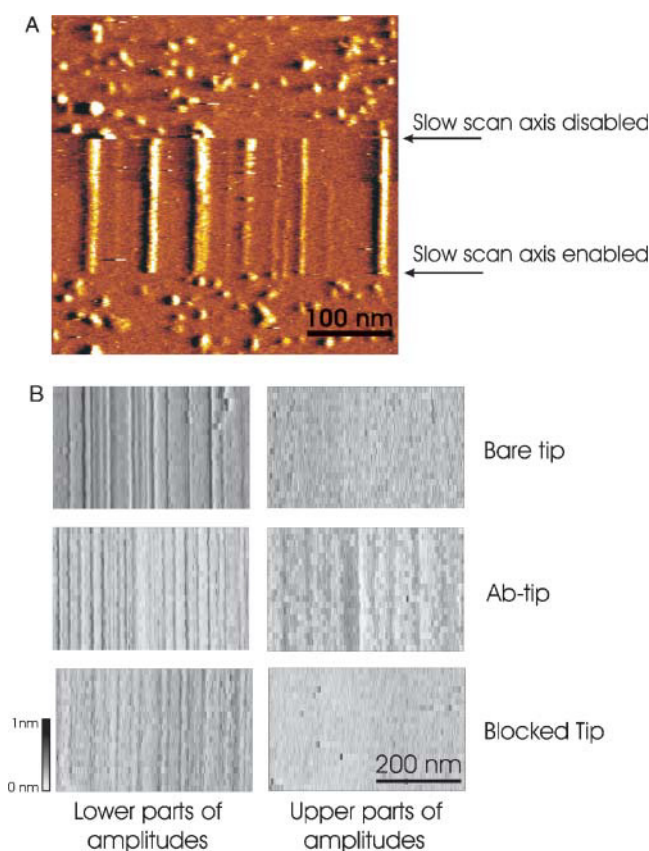


FIGURE 6 (A) Principle of recording repetitive traces while scanning lysozyme molecules adsorbed onto mica surfaces. (B) The slow scan axis was disabled and the deflection signal was recorded on a sound card. Minima (left panels) and maxima (right panels) of the oscillation amplitudes were depicted using MATLAB. The traces are shown in false color gray code (see height bar, 0–1 nm) over a full scan line (500 nm).

~1 nm in height and 10–15 nm in width were clearly observed (Fig. 6 A). The slow scan axis was then disabled and the tip oscillation was recorded, so that it repetitively followed the signals belonging to the same molecules in one scan line. After several lines had been recorded, the slow scan axis was enabled and single lysozyme molecules were visible again. The oscillation signals were analyzed and the minima and maxima of each single oscillation period were plotted along repetitive scan axes (from *top* to *bottom*), resulting in the images shown in Fig. 6 B.

This method was applied for bare tips (Fig. 6 B, *upper panel*), and antibody-conjugated tips in buffer solutions lacking (Fig. 6 B, *middle panel*) and containing free HyHEL5-antibody (Fig. 6 B, *lower panel*), respectively. The three left panels, which contain the oscillation minima providing the topographical signals, all showed variations very similar in shape. The appearance of highly ordered “stripes” arising from consecutive cross sections of the height profile (top to bottom) of the same molecules reflects the good reproducibility of the topographic signals. Utilizing the same three kinds of tips that were used for the topography

panels (Fig. 6 B, *left*), the maxima of the oscillations that contain the recognition signals are shown (Fig. 6 B, *right*). An amplitude reduction in the upper oscillations of ~1 nm (see *height bar* in Fig. 6 B) was only visible when a functional antibody on the tip was used on unblocked lysozyme molecules (*middle panel*). Both bare tip (*upper right panel*) and an antibody-carrying tip probing blocked lysozyme molecules (*lower right panel*) did not show any recognition events. Thus, the signals observed in the right middle panel must arise from the specific binding of an antibody on the AFM tip to lysozyme molecules on the surface. The ordered appearance (stripe-like features in repetitive scans) is a conceptual prove for the reproducibility obtained by the recognition measurements. The specificity of binding is evident from the lack of recognition events in the block experiment (*lower right panel*).

Simultaneous imaging of topography and recognition

Topography and recognition images were simultaneously obtained using a homebuilt electronic circuit (Fig. 7). Maxima (U_{up}) and minima (U_{down}) of each sinusoidal cantilever deflection period were depicted in a peak detector, filtered, and amplified. DC offset signals were used to compensate for the thermal drifts of the cantilever. U_{up} and U_{down} were fed into the AFM controller via a breakout box, with U_{down} driving the feedback loop to record the height (i.e., topography) image and U_{up} providing the data for constructing the recognition image. Since we used cantilevers with low Q-factor (~1 in liquid) driven at frequencies below resonance, both types of information were independent. In this way, topography and recognition image were recorded simultaneously and independently.

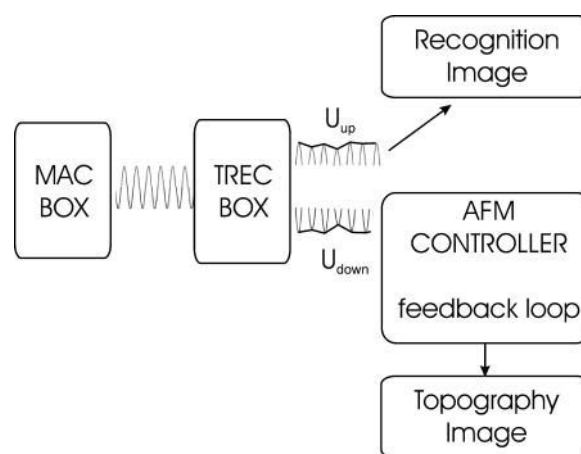


FIGURE 7 Signal processing for simultaneously obtaining topography and recognition images. The raw cantilever deflection signal obtained in the MACmode is fed into the TREC box, where the maxima (U_{up}) and minima (U_{down}) of each oscillation period are depicted and used for the recognition and topography image, respectively.

The circuit was applied to mica containing singly distributed lysozyme molecules. The sample was imaged with an antibody containing tip, yielding the topography (Fig. 8 A) and the recognition image (Fig. 8 B) at the same time. The tip oscillation amplitude (5 nm) was chosen to be slightly smaller than the extended cross-linker length, so that both the antibody remained bound while passing a binding site and the reduction of the upwards deflection was of sufficient significance compared to the thermal noise. Since the spring constant of the polymeric cross-linker increases nonlinearly with the tip-surface distance (Fig. 3), the binding force is only sensed close to full extension of the cross-linker (given at the maxima of the oscillation period). Therefore, the recognition signals were well separated from the topographic signals arising from the surface, both in space ($\Delta z \sim 5$ nm) and time (half oscillation period ~ 0.1 ms).

The bright dots with 2–3 nm in height and 15–20 nm in diameter visible in the topography image (Fig. 8 A) represent single lysozyme molecules stably adsorbed onto the flat mica surface (Raab et al., 1999). The recognition image shows black dots at positions of lysozyme molecules (Fig. 8 B) because the oscillation maxima are lowered due to the physical lysozyme-antibody connection established during recognition (cf. also Figs. 5 and 6). Roughly two-thirds of the lysozyme molecules visible in the topography image are recognized by the antibody-modified tip in the recognition image at a high signal-to-noise ratio (indicated with *black arrows* in Fig. 8). Apparently, recognition between the antibody on the tip and the lysozyme on the surface was observed with high frequency (i.e., $\sim 70\%$ efficiency), most likely because both the region of lysozyme close to the antibody binding epitope and the mica surface are negatively charged. Thus, one would assume to have almost all binding epitopes oriented away from the mica surface and accessible to the antibody on the tip, resulting in the high binding efficiency observed before (Raab et al., 1999).

In addition, the tether length via which the antibody was bound to the AFM tip was greater (8 nm) than the oscillation amplitude (5 nm) so that the antibody on the tip always had a chance to bind to the antigen when passing an antigenic site during lateral scans. Antibody-antigen recognition resulted in a reduction of the oscillation amplitude and, indeed, due to

the close proximity of the tip to the surface the binding efficiency was high. It is important to note that topography and recognition images were recorded at speeds typical for standard AFM imaging and were therefore considerably faster than conventional force mapping.

CONCLUSIONS

Lysozyme molecules adsorbed onto mica surfaces remained stably bound during MAC mode imaging, most likely, because of the strong electrostatic interaction between the positively charged lysozyme and the negatively charged mica. Consequently, single molecules were clearly resolved in topographic images. Furthermore, EIA revealed that the suchlike adsorbed lysozymes were functionally active to HyHEL5-antibody binding. A high efficiency was obtained using a single molecule preparation on mica, indicating that most of the lysozyme molecules are functional with respect to antibody binding. The latter finding is not unexpected because both mica and the region close to the HyHEL5-antibody binding epitope of lysozyme are negatively charged. Thus, one would assume to have the binding epitopes directed away from the mica surface and therefore accessible for HyHEL5 (Raab et al., 1999).

Molecular recognition between lysozyme on the mica surface and antilysozyme antibody (HyHEL5) on a tip was then studied using force microscopy. Single molecule unbinding events were resolved in force-distance cycles, revealing an unbinding force of ~ 60 pN. The specificity of binding was confirmed by blocking with free antibody in solution. Since a distensible 8-nm long linker (PEG) was used to couple HyHEL5 to the AFM tip, the antibodies were spaced from the tip surface and unbinding occurred several nm away from the tip-surface contact point. Thus, recognition was separated from the topography information and can be clearly distinguished from unspecific tip-sample interaction.

Different modes were employed to localize lysozyme/HyHEL5 interaction sites using a HyHEL5-antibody tethered to the AFM tip and a single molecule lysozyme preparation on mica. In force mapping images antigenic binding sites were detected and the specificity was confirmed

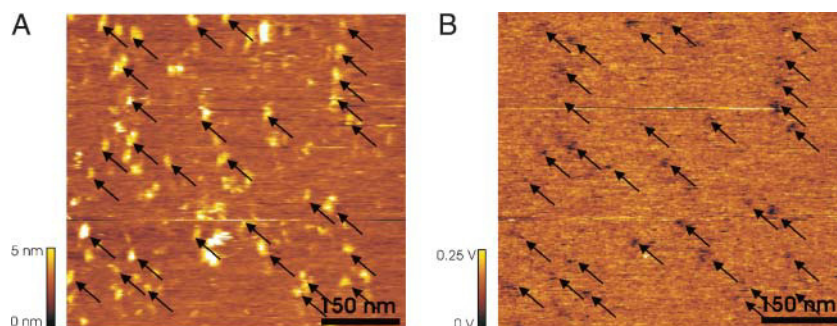


FIGURE 8 Simultaneously acquired topography (A) and recognition (B) image using a HyHEL5 antibody-coated tip on lysozyme molecules adsorbed onto mica surface. (A) Topography image showing single lysozyme molecules. (B) Recognition image. The black dots indicate positions of antigenic sites. The correlation between topography and recognition image is indicated with black arrows, showing that at least two-thirds of the lysozyme molecules are recognized in the recognition image at the same position.

by blocking the lysozyme molecules on the surface with free antibody in solution. Going to the limit of speed for recording unbinding forces in force-distance cycles in aqueous solutions using commercially available cantilevers (10 Hz at 100 nm sweep length), a 64×64 pixel image was recorded in 14 min. Therefore this mode lacks high lateral resolution at reasonable data acquisition times. In addition, the topography of single molecules is not attainable, so that structure-function relations cannot be achieved.

To overcome the limitations of force mapping, dynamic force microscopy was employed, which can be operated at considerably higher frequencies. Initial line trace experiments helped us to understand the effects of topographical changes and recognition on the cantilever oscillations using the magnetic AC mode. The results clearly indicate that at the conditions used in our experiments (cantilever spring constant 0.1 N/m; Q-factor ~ 1 ; resonance frequency ~ 7 kHz) the surface topography affects only the lower parts (minima; regions that are intermittently in contact with the sample surface) of the oscillation. In contrast, recognition affects only the upper parts (maxima), provided that the oscillation amplitude is carefully adjusted (i.e., slightly less than the cross-linker length via which the antibody is conjugated to the tip).

A special electronic box was built to separate minima and maxima. The minima were used to drive the feedback loop for obtaining a topography image, and the maxima revealed the information for the simultaneously recorded recognition image. Recognition was only detected when an antibody-conjugated tip was used. With this method, topography and recognition image were recorded at single molecule resolution at time scales equivalent to standard AFM imaging times (512×512 pixels in 8 minutes). Since both informations were acquired at the same time binding sites can be assigned to molecular structures, which opens a wide field of applications for investigating structure-function relationships in aqueous environments on the nanometer scale.

This work was supported by the Austrian Science Funds projects P12802/14549/15295 and the GEN-AU initiative of the Austrian Ministry of Education, Science and Culture.

REFERENCES

- Almqvist, N., R. Bhatia, G. Primbs, N. Desai, S. Banerjee, and R. Lal. 2004. Elasticity and adhesion force mapping reveals real-time clustering of growth factor receptors and associated changes in local cellular rheological properties. *Biophys. J.* 86:1753–1762.
- Baumgartner, W., P. Hinterdorfer, W. Ness, A. Raab, D. Vestweber, H. Schindler, and D. Drenckhahn. 2000a. Cadherin interaction probed by atomic force microscopy. *Proc. Natl. Acad. Sci. USA.* 97:4005–4010.
- Baumgartner, W., P. Hinterdorfer, and H. Schindler. 2000b. Data analysis of interaction forces measured with the atomic force microscope. *Ultramicroscopy.* 82:85–95.
- Binnig, G., C. F. Quate, and C. Gerber. 1986. Atomic force microscope. *Phys. Rev. Lett.* 56:930–933.
- Butt, H. J., and M. Jaschke. 1995. Calculation of thermal noise in atomic force microscopy. *Nanotechnology.* 6:1–7.
- Evans, E., and K. Ritchie. 1997. Dynamic strength of molecular adhesion bonds. *Biophys. J.* 72:1541–1555.
- Fisher, T. E., A. F. Oberhauser, M. Carrion-Vazquez, P. E. Marszalek, and J. M. Fernandez. 1999. The study of protein mechanics with the atomic force microscope. *TIBS.* 4:379–384.
- Florin, E. L., V. T. Moy, and H. E. Gaub. 1994. Adhesion forces between individual ligand-receptor pairs. *Science.* 264:415–417.
- Fritz, J., A. G. Katopodis, F. Kolbinger, and D. Anselmetti. 1998. Force mediated kinetics of single P-selectin/PSGL-1 complexes observed by AFM. *Proc. Natl. Acad. Sci. USA.* 95:12283–12288.
- Grandbois, M., W. Dettmann, M. Benoit, and H. E. Gaub. 2000. Affinity imaging of red blood cells using an atomic force microscope. *J. Histochem. Cytochem.* 48:719–724.
- Grubmueller, H., B. Heymann, and B. Tavan. 1996. Ligand binding and molecular mechanics calculation of the streptavidin-biotin rupture force. *Science.* 271:997–999.
- Han, W., S. M. Lindsay, and T. A. Jing. 1996. A magnetically driven oscillating probe microscope for operation in liquid. *Appl. Phys. Lett.* 69:1–3.
- Han, W., S. M. Lindsay, M. Dlakic, and R. E. Harrington. 1997a. Kinked DNA. *Nature.* 386:563.
- Han, W., M. Dlakic, Y. J. Zhu, S. M. Lindsay, and R. E. Harrington. 1997b. Strained DNA is kinked by low concentrations of Zn. *Proc. Natl. Acad. Sci. USA.* 94:10565–10570.
- Haselgruebler, T., A. Amerstorfer, H. Schindler, and H. J. Gruber. 1995. Synthesis and application of a new poly(ethylene glycol) derivative for the cross-linking of amines with thiols. *Bioconjugate Chem.* 6:242–248.
- Hinterdorfer, P., W. Baumgartner, H. J. Gruber, K. Schilcher, and H. Schindler. 1996. Detection and localization of individual antibody-antigen recognition events by atomic force microscopy. *Proc. Natl. Acad. Sci. USA.* 93:3477–3481.
- Hinterdorfer, P., K. Schilcher, W. Baumgartner, H. J. Gruber, and H. Schindler. 1998. A mechanistic study of the dissociation of individual antibody-antigen pairs by atomic force microscopy. *Nanobiology.* 4: 39–50.
- Hutter, J. L., and J. Bechhoefer. 1993. Calibration of atomic-force microscope tips. *Rev. Sci. Instrum.* 64:1868–1873.
- Jena, B. P., and H. K. Hoerber. 2002. *Methods in Cell Biology* 68. Academic Press.
- Kienberger, F., G. Kada, H. J. Gruber, V. P. Pastushenko, C. Riener, M. Trieb, H.-G. Knaus, H. Schindler, and P. Hinterdorfer. 2000a. Recognition force spectroscopy studies of the NTA-His₆ bond. *Single Mol.* 1:59–65.
- Kienberger, F., V. P. Pastushenko, G. Kada, H. J. Gruber, C. Riener, H. Schindler, and P. Hinterdorfer. 2000b. Static and dynamical properties of single poly(ethylene glycol) molecules investigated by force spectroscopy. *Single Mol.* 1:123–128.
- Kienberger, F., C. Stroh, G. Kada, R. Moser, W. Baumgartner, V. Pastushenko, C. Rankl, U. Schmidt, H. Muller, E. Orlova, C. LeGrimellec, D. Drenckhahn, D. Blaas, and P. Hinterdorfer. 2003. Dynamic force microscopy imaging of native membranes. *Ultramicroscopy.* 97:229–237.
- Lantz, M., Y. Z. Liu, X. O. Cui, H. Tokumoto, and S. M. Lindsay. 1999. Dynamic force microscopy in fluid. *Surf. Interface Anal.* 27:354–360.
- Lee, G. U., D. A. Kidwell, and R. J. Colton. 1994. Sensing discrete streptavidin-biotin interaction with the atomic force microscope. *Langmuir.* 10:354–357.
- Lehenkari, P. P., G. T. Charras, A. Nykaenen, and M. A. Horton. 2000. Adapting atomic force microscopy for cell biology. *Ultramicroscopy.* 82:289–295.
- Ludwig, M., W. Dettmann, and H. E. Gaub. 1997. AFM imaging contrast based on molecular recognition. *Biophys. J.* 72:445–448.

- Merkel, R., P. Nassoy, A. Leung, K. Ritchie, and E. Evans. 1999. Energy landscapes of receptor ligand bonds explored with dynamic force spectroscopy. *Nature*. 397:50–53.
- Mizes, H. A., K.-G. Loh, R. J. D. Miller, S. K. Ahuja, and E. F. Grabowski. 1991. Submicron probe of polymer adhesion with atomic force microscopy: dependence on topography and material inhomogeneities. *Appl. Phys. Lett.* 59:2901–2903.
- Oberhauser, A. F., P. E. Marszalek, H. P. Erickson, and J. M. Fernandez. 1998. The molecular elasticity of the extracellular matrix tenascin. *Nature*. 393:181–185.
- Periasamy, A. 2001. *Methods in Cellular Imaging*. Oxford University Press, Oxford, UK.
- Raab, A., W. Han, D. Badt, S. J. Smith-Gill, S. M. Lindsay, H. Schindler, and P. Hinterdorfer. 1999. Antibody recognition imaging by force microscopy. *Nat. Biotechnol.* 17:902–905.
- Radmacher, M., J. P. Cleveland, M. Fritz, H. G. Hansma, and P. K. Hansma. 1994. Mapping interaction forces with the atomic force microscope. *Biophys. J.* 66:2159–2165.
- Rief, M., M. Gautel, F. Oesterhelt, J. M. Fernandez, and H. E. Gaub. 1997. Reversible unfolding of individual titin immunoglobulin domains by AFM. *Science*. 276:1109–1112.
- Riener, C. K., F. Kienberger, C. D. Hahn, G. M. Buchinger, I. O. C. Egwim, T. Haselgruebler, A. Ebner, C. Romanin, C. Klampfl, B. Lackner, H. Prinz, D. Blaas, P. Hinterdorfer, and H. J. Gruber. 2003. Heterobifunctional cross-linkers for tethering single ligand molecules to scanning probes. *Anal. Chime. Acta*. 497:101–114.
- Ros, R., F. Schwesinger, D. Anselmetti, M. Kubon, R. Schaefer, A. Plueckthun, and L. Tiefenauer. 1998. Antigen binding forces of individually addressed single-chain Fv antibody molecules. *Proc. Natl. Acad. Sci. USA*. 95:7402–7405.
- Schaffer, T. E., and J. Yuekan. 2001. High-speed force mapping using small cantilevers. *Biophys. J.* 80:303.
- Schindler, H., D. Badt, P. Hinterdorfer, F. Kienberger, A. Raab, S. Wielert-Badt, and V. P. Pastushenko. 2000. Optimal sensitivity for molecular recognition MACmode AFM. *Ultramicroscopy*. 82:227–235.
- Schwesinger, F., R. Ros, T. Strunz, D. Anselmetti, H.-J. Guentherodt, A. Honegger, L. Jermutus, L. Tiefenauer, and A. Plueckthun. 2000. Unbinding forces of single antibody-antigen complexes correlate with their thermal dissociation rates. *Proc. Natl. Acad. Sci. USA*. 97:9972–9977.
- Silverton, E. W., M. A. Navia, and D. Davies. 1977. Three-dimensional structure of an intact human immunoglobulin. *Proc. Natl. Acad. Sci. USA*. 74:5140–5144.
- Strunz, T., K. Oroszlan, R. Schaefer, and H.-J. Guentherodt. 1999. Dynamic force spectroscopy of single DNA molecules. *Proc. Natl. Acad. Sci. USA*. 96:11277–11282.
- van der Werf, K. O., C. A. J. Putman, B. G. de Grooth, and J. Greve. 1994. Adhesion force imaging in air and liquid by adhesion mode atomic force microscopy. *Appl. Phys. Lett.* 65:1195–1197.
- Viani, B. V., T. E. Schaeffer, A. Chand, M. Rief, H. E. Gaub, and P. K. Hansma. 1999. Small cantilevers for force spectroscopy of single molecules. *J. Appl. Phys.* 86:2258–2262.
- Willemsen, O. H. E., M. M. Snel, K. O. van der Werf, B. G. de Grooth, J. Greve, P. Hinterdorfer, H. J. Gruber, H. Schindler, Y. van Kooyk, and C. G. Figdor. 1998. Simultaneous height and adhesion imaging of antibody-antigen interactions by atomic force microscopy. *Biophys. J.* 75:2220–2228.
- Yuan, C., A. Chen, P. Kolb, and V. T. Moy. 2000. Energy landscape of avidin-biotin complexes measured by atomic force microscopy. *Biochemistry*. 39:10219–10223.